Flange Bending in Single Curvature

BO DOWSWELL

ABSTRACT

Local bending of beam and column flanges is a common design consideration in steel structures. In most cases, the flange bends in double curvature due to the restraining effect of the connecting element. When a restraining force is not present, the flange will deform in single curvature. Common cases of single-curvature bending occur at the bottom flange of monorail beams and at hanger rod connections. In this paper, the equivalent-width method was explored in an effort to determine design procedures for elastic and plastic strength of flanges in single-curvature bending.

This paper compares the available procedures for designing flanges bent in single curvature. New finite element models and yield line analyses are used to verify, expand and improve the existing design methods. Design recommendations are made for both elastic and ultimate strength approaches. Recommendations are also made for interaction of the local bending strength with longitudinal stresses in the flange. The effects of closely spaced loads and loads acting near the ends of members are also addressed.

Keywords: flange bending, design recommendations.

INTRODUCTION

Local bending of beam and column flanges is a common design consideration in steel structures. Flange bending usually occurs when a tension member is bolted to the flange as shown in Figure 1a. In this case, the flange bends in double curvature due to the restraining effect of the connecting element. When a restraining force is not present, the flange will deform in single curvature as shown in Figure 1b. Common cases of single-curvature bending occur at the bottom flange of monorail beams and at hanger connections as shown in Figures 2a and 2b, respectively.

Geometry is the dominant factor in the behavior of bolted flange connections. Another major factor is the amount of inelastic deformation that can be tolerated before serviceability requirements are exceeded. The monorail beam flange in Figure 2a must remain essentially elastic under service loads. Conversely, the strength of the hanger connection in Figure 2b can normally be calculated on the basis of a fully plastic yield line solution. Additionally, it may be practical to use an ultimate strength approach when calculating the strength of a monorail flange to ensure safety at overload conditions.

Figure 3 shows a generic load versus deformation curve for flanges bent in single curvature. The curve is linear up to the elastic load, P_e. After yielding, the curve is nonlinear over a large increment of the total load, and then the curve flattens out and becomes essentially linear until collapse. The inelastic load, P_i, is at the intersection of the elastic loading line and the plastic loading line. Tests and inelastic finite element results summarized by Dowswell (2011) indicate that P_i is generally 60 to 70% greater than the initial yield load, P_e. The plastic collapse load, P_c, can be more than four times the initial yield load; however, Dowswell also showed that the deformation will be approximately ¼ in. at the nominal load calculated with the yield line method.

When a concentrated load is applied to the flange, bending stresses develop in two directions. Because the stresses in the longitudinal direction (Z-axis in Figure 2a) are much smaller than those in the transverse direction (X-axis in Figure 2a), the stresses in the longitudinal direction are often neglected in design. A simple method to calculate the stresses in the transverse direction is the equivalent-width method. In the equivalent-width method, the flange is treated as a rectangular cantilever beam of width, b_e, based on an assumed load distribution angle, θ, as shown in Figure 4. Goldman (1990) recommended a load distribution angle of 45°, which results in an equivalent width of 2*b*. Although the 45° angle is common for design use, this paper shows that the equivalent width is dependent on the *b*/*c* ratio and the level of inelasticity.

The equivalent-width method will be explored in an effort to determine procedures for elastic and plastic design of flanges in single-curvature bending. The effects of closely spaced loads and loads acting near the ends of the member will also be addressed.

Using the equivalent-width approach, the required moment is

$$M_r = Pb \tag{1}$$

Bo Dowswell, P.E., Ph.D., Principal, ARC International, LLC, Birmingham, AL.
E-mail: bo@arcstructural.com

For design of flanges that must remain elastic, the nominal yield moment is

$$M_n = S_e F_y \tag{2}$$

$$S_e = \frac{b_e t_f^2}{6} \tag{3}$$

When the plastic strength is used, the nominal moment is

$$M_n = Z_e F_y \tag{4}$$

$$Z_e = \frac{b_e t_f^2}{4} \tag{5}$$

where

F_y = specified minimum yield stress, ksi
P = concentrated force, kips
S_e = section modulus of the equivalent beam, in.^{3}
Z_e = plastic modulus of the equivalent beam, in.^{3}

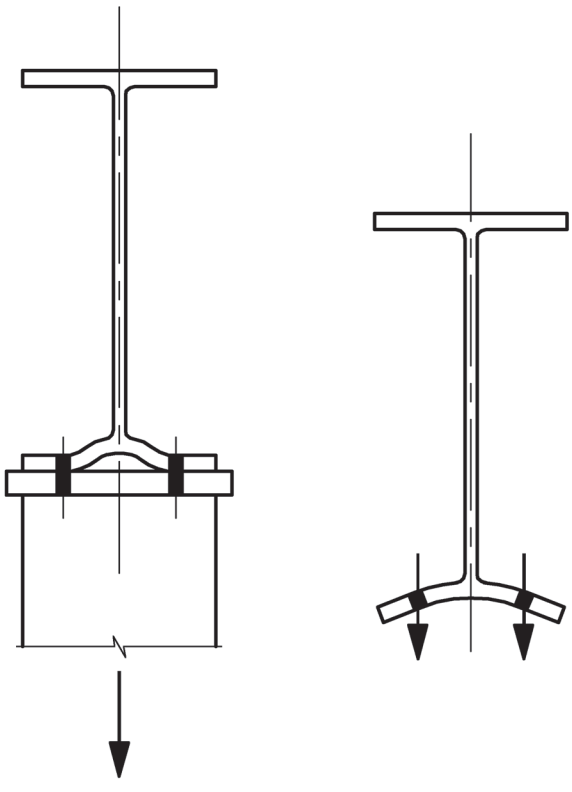

(a) (b)

Fig. 1. Effect of restraint on flange bending: (a) double curvature; (b) single curvature.

b = distance from the concentrated load to the fixed end of the equivalent beam, in.
b_e = equivalent width, in.
t_f = flange thickness, in.

ELASTIC STRESSES

In this section, the previous research on elastic bending stresses in flanges will be summarized. The equivalent-width equations discussed are for use with the section modulus, and the nominal strength is calculated with Equation 2.

Jaramillo (1950)

The first research was published by Jaramillo (1950), who transformed the exact solution into series form and solved for the moments in an infinitely long plate with one edge fixed and the other edge free. The results were presented in the form of a table, which was reproduced in Young (1989). The equivalent width is calculated using Equation 6 with the values for K_m listed in Table 1.

$$b_e = \frac{b}{K_m} \tag{6}$$

Timoshenko and Woinowsky-Krieger (1959) published the solution for an infinitely long plate fixed at one edge and free at the other edge with a concentrated load at the free edge. The unit moment causing bending stress perpendicular to the length of the beam is

$$m_z = 0.509P \tag{7}$$

The unit moment causing bending stress parallel to the length of the beam is

$$\begin{aligned} m_x &= \nu m_z \\ &= 0.153P \end{aligned} \tag{8}$$

The equivalent width can be determined by combining Equations 1 and 7.

$$\begin{aligned} b_e &= \frac{M_r}{m_z} \\ &= \frac{Pb}{m_z} \\ &\approx 2b \end{aligned} \tag{9}$$

This results in a load distribution angle of 45°, which is the same as Jaramillo (1950) when $b/c = 1$.

Table 1. Bending Coefficients According to Jaramillo (1950)	
b/c	***K_m***
0.25	0.332
0.50	0.370
0.75	0.428
1.00	0.509

Ballio and Mazzolani (1983)

Ballio and Mazzolani (1983) presented the results of a finite element study aimed at generalizing the solution of Timoshenko and Woinowsky-Krieger (1959). They published Equation 10 for calculating the equivalent width.

$$b_e = b\left(3.5 - 1.5\frac{b}{c}\right) \tag{10}$$

where

c = horizontal distance from the face of the web to the tip of the flange, in.

Current Study

To supplement the previous research, the problem was modeled by the author using elastic finite element models with rectangular plate elements. The plate was fixed at one boundary and free at the remaining three edges. It was determined that a length of five times the width was adequate to model an infinitely long plate in the elastic range. The mesh size was chosen to provide a convenient number of equally spaced load points. However, a mesh study revealed that the element size provided convergence within 2%.

The results are presented in the same form as Jaramillo (1950), and the equivalent width can be calculated using Equation 6 with the values for K_m listed in Table 2. The results agree well with those of Jaramillo (1950), Timoshenko and Woinowsky-Krieger (1959) and Ballio and Mazzolani (1983).

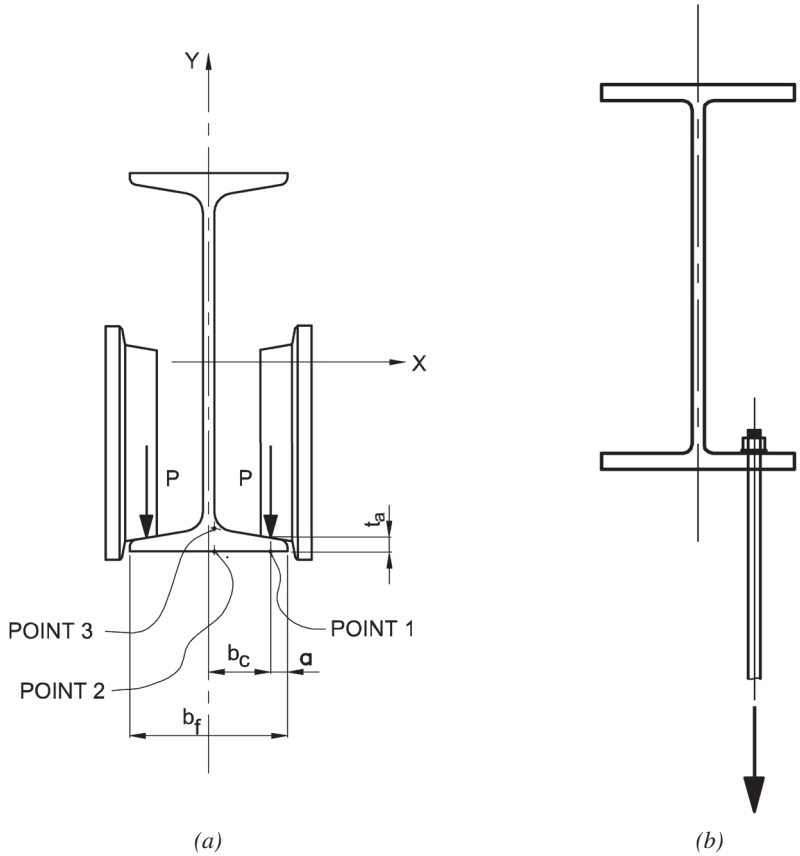

Fig. 2. Common cases of flange bending in single curvature: (a) monorail; (b) hanger.

Table 2. Bending Coefficients According to Current Study	
b/c	K_m
0.125	0.252
0.250	0.312
0.375	0.337
0.500	0.363
0.625	0.392
0.750	0.426
0.875	0.464
1.00	0.508

INELASTIC STRENGTH

In this section, the research on inelastic bending strength of flanges are summarized. The equivalent-width equations discussed are for use with the plastic modulus, and the nominal strength is calculated with Equation 4.

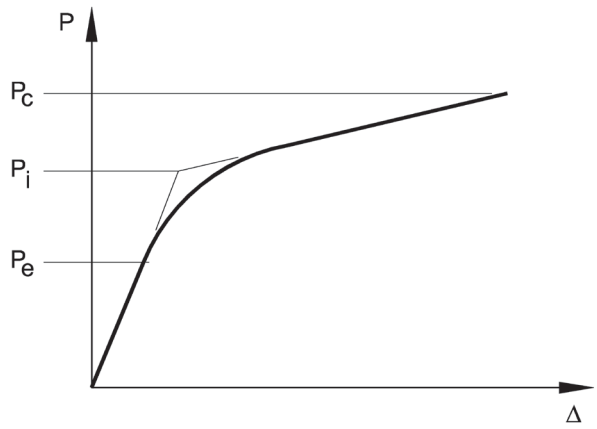

Fig. 3. Load versus deformation curve.

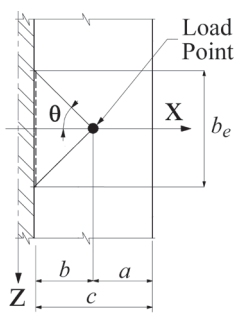

Fig. 4. Equivalent-width approach.

Ballio, Poggi and Zanon (1981)

Ballio, Poggi and Zanon (1981) used experimental tests on monorail beams and inelastic finite element models of long plates with one edge fixed and three edges free. The suggested design equations contain variables for the load application width, assuming a uniform load over a finite-width patch. For a concentrated load, the width of the load is zero, and the equivalent width is calculated with Equation 11.

$$b_e = b\left(9 - 6\frac{b}{c}\right) \tag{11}$$

Equation 11 was derived to provide a target nominal strength at the intersection of the elastic loading line and the plastic loading line as labeled P_i in Figure 3 when used with the plastic modulus.

PLASTIC STRENGTH

In this section, the available yield line patterns for single-curvature bending of flanges are summarized. The equivalent-width equations discussed are for use with the plastic modulus, and the nominal strength is calculated with Equation 4.

Triangular Yield Line Pattern (Dranger, 1977)

Dranger (1977) derived an equation for the flange strength using the yield line pattern of Figure 5. The nominal load is

$$P_n = F_y t_f^2 \sqrt{2}\left(\frac{c}{b}\right) \tag{12}$$

Combining Equations 1, 4 and 12, the equivalent width is

$$b_e = 4c\sqrt{2} \tag{13}$$

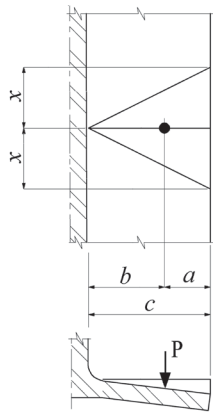

Fig. 5. Triangular yield line pattern.

Parabolic Yield Line Pattern (Otegui, 1996)

Based on earlier work on curved yield line patterns by Packer and Morris (1977) and Mann and Morris (1979), Otegui (1996) derived the flange bending strength of a tee stub with bolts near the end, as shown in Figure 6. Otegui used a parabolic pattern with an experimentally located distance from the focal point to the vertex of 2.17*b*. He showed that the internal work is independent of the radius of the yield line pattern; therefore, the radius can vary around the arc of the curve, but the internal work is dependent on the total angle of the parabola. Another important concept in Otegui's derivation is that the work done along the curved yield lines is equal to that of the straight yield lines projecting from the center of the load point.

The strength of the yield line pattern in Figure 7 can be derived based on the principles developed by Otegui. The external work is

$$W_e = P\delta \tag{14}$$

where

δ = virtual displacement of the load

The internal work is

$$W_i = 4m_p\alpha\delta \tag{15}$$

where

m_p = plastic moment capacity per unit length, kips

α = half angle around the parabola (Figure 7), radians

The plastic capacity per unit length of yield line is

$$m_p = \frac{F_y t_f^2}{4} \tag{16}$$

The half angle around the parabola is

$$\alpha = \frac{\pi}{2} + \beta \tag{17}$$

where

$$\tan\beta = \frac{a}{x} \tag{18}$$

Dimensions a and x are shown in Figure 7.

From Otegui (1996),

$$x = 3\sqrt{bc} \tag{19}$$

Set $W_e = W_i$ and substitute m_p from Equation 16 to get the nominal load

$$P_n = F_y\, t_f^2\, \alpha \tag{20}$$

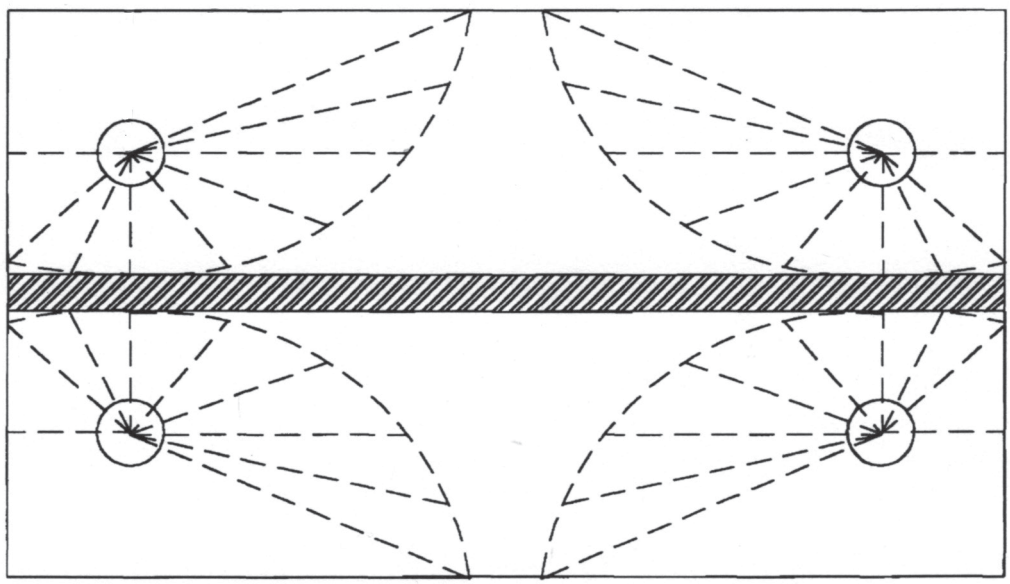

Fig. 6. Yield line pattern of Otegui (1996).

Equation 17 is substituted into Equation 20 to get the final design equation

$$P_n = F_y t_f^2 \left[\frac{\pi}{2} + \beta\right] \tag{21}$$

Equation 19 can be substituted into Equation 18 to get

$$\tan\beta = \frac{a}{3\sqrt{bc}} \tag{22}$$

Combining Equations 1, 4 and 21, the equivalent width is

$$b_e = 4b\left(\frac{\pi}{2} + \beta\right) \tag{23}$$

REVIEW OF MONORAIL DESIGN SPECIFICATIONS

In this section, the available monorail design specifications will be summarized. Because the beam flange must remain essentially elastic, the equivalent-width equations discussed are for use with the section modulus and the nominal strength is calculated with Equation 2.

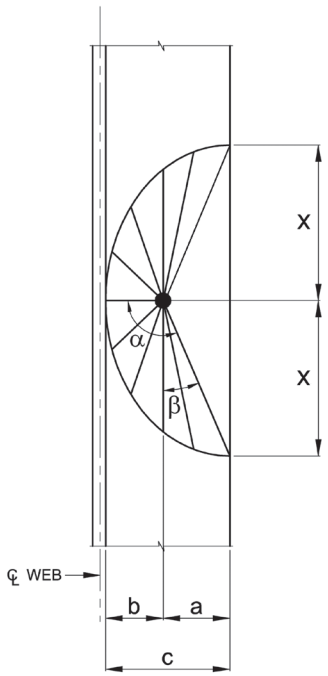

Fig. 7. Parabolic yield line pattern.

CMAA Specification

CMAA *Specification* (CMAA, 2008) Section 3.3.2.4 contains detailed design provisions for calculation of flexural normal stresses in directions parallel and perpendicular to the longitudinal axis of the beam. The rules were taken from FEM (1983), with the development and background research by Hannover and Reichwand (1982). Hannover and Reichwand developed the equations by curve-fitting data from experimental tests, finite element models, and theoretical calculations using Kirchoff's plate theory. The notation in the design equations reproduced here is shown in Figure 2a.

Stresses at point 1

$$\sigma_{x1} = C_{x1}\left(\frac{P}{t_a^2}\right) \tag{24}$$

$$\sigma_{z1} = C_{z1}\left(\frac{P}{t_a^2}\right) \tag{25}$$

Stresses at point 2

$$\sigma_{x2} = C_{x2}\left(\frac{P}{t_a^2}\right) \tag{26}$$

$$\sigma_{z2} = C_{z2}\left(\frac{P}{t_a^2}\right) \tag{27}$$

Stresses at point 3

$$\sigma_{x3} = -\sigma_{x2} \tag{28}$$

$$\sigma_{z3} = -\sigma_{z2} \tag{29}$$

For tapered flange sections

$$t_a = t_f - \frac{b_f}{24} + \frac{a}{6} \tag{30}$$

$$C_{x1} = 3.97 - 4.84\lambda - 3.97e^{-2.68\lambda} \tag{31}$$

$$C_{x2} = -1.10 + 1.10\lambda + 0.192e^{-6.00\lambda} \tag{32}$$

$$C_{z1} = 1.81 - 1.15\lambda - 1.06e^{-7.70\lambda} \tag{33}$$

$$C_{z2} = -0.981 - 1.48\lambda + 1.12e^{1.32\lambda} \tag{34}$$

For parallel flanged sections

$$t_a = t_f \tag{35}$$

$$C_{x1} = 10.1 - 7.41\lambda - 10.1e^{-1.36\lambda} \tag{36}$$

$$C_{x2} = -2.11 + 1.98\lambda + 0.0076e^{6.53\lambda} \tag{37}$$

$$C_{z1} = 2.23 - 1.49\lambda - 1.39e^{-18.3\lambda} \tag{38}$$

$$C_{z2} = 0.050 - 0.580\lambda + 0.148e^{3.02\lambda} \tag{39}$$

where

$$\lambda = \frac{2a}{b_f - t_w} = \frac{a}{c} \tag{40}$$

t_a = beam flange thickness at the point of load application, in.
= t_f for parallel flange sections
t_w = web thickness, in.
b_f = flange width, in.
a = distance from the edge of the flange to the point of load application, in.

For parallel flanged sections, the equivalent width can be determined by substituting σ_{x2} from Equation 26 for F_y in Equation 2, and combining with Equations 1 and 3, which results in Equation 41.

$$b_e = \frac{6b}{C_{x2}} \tag{41}$$

Australian Standard AS 1418.18-2001

Australian Standard AS 1418.18-2001 (AS, 2001) Section 5.12.3.1 specifies Equation 42 to calculate the allowable wheel load for the limit state of local flange bending. In order to use consistent terminology and units throughout this paper, some of the constants and variable names were changed from the original equation.

$$P_a = K_L t_f^2 \left(\frac{\alpha F_y}{1 + 8b_c/b_f} \right) \tag{42}$$

where

P_a = allowable wheel load, kips
K_L = load position factor
= 1.7 where the distance from the end of the beam to the wheel load is at least $b_f + d$
= 1.0 where the distance from the end of the beam to the wheel load is less than $b_f + d$
b_c = horizontal distance from the center of the beam to the wheel load, in.
b_f = beam flange width, in.
d = beam depth, in.
α = reduction factor to account for longitudinal stress in the bottom flange due to global bending of the beam

For comparison with the other design equations, $K_L = 1.7$ and $\alpha = 1.0$ are substituted into Equation 42, which then reduces to Equation 43.

$$P_a = \frac{1.7F_y t_f^2}{1 + 8b_c/b_f} \tag{43}$$

Combining Equations 1, 2 and 43, assuming a safety factor of 1.67, and neglecting the web thickness, the equivalent width is

$$b_e = \frac{17b}{1 + 4b/c} \tag{44}$$

Eurocode 1993-6

For design at service loads, Eurocode (1999) specifies the same equations as CMAA *Specification* (CMAA, 2008) Section 3.3.2.4. For ultimate strength design, Eurocode specifies the equations developed by Dranger (1977), except that the critical section for bending is assumed to be at the tangent point of the fillet radius instead of the face of the web. For wheel loads remote from the end of the member and at large enough spacings to preclude interaction between any adjacent yield lines, the available load for strength design is

$$P_a = \frac{b_e \, t_f^2 \, \alpha F_y}{4b'\gamma} \tag{45}$$

where

$$b_e = 4c'\sqrt{2} \tag{46}$$

b' = horizontal distance from the tangent point of the fillet radius to the concentrated load, in.
= $b - r$
c' = horizontal distance from the tangent point of the fillet radius to the tip of the flange, in.
= $c - r$

r = fillet radius, in.
γ = partial safety factor for LRFD design
= 1.1

SUMMARY AND CONCLUSIONS FOR EQUIVALENT-WIDTH EQUATIONS

Comparison of Equivalent-Width Equations

Figure 8 shows a plot of the normalized equivalent width, b_e/b, versus the normalized load location, a/c, for each of the equivalent-width equations discussed in this paper. All of the equivalent-width equations are for parallel flanged sections; therefore, the CMAA (2008) curve used Equation 37 to calculate C_{x2}.

The equivalent-width equations are separated into three groups: elastic (green line), inelastic (red lines) and plastic (blue lines). Figure 8 shows that the curves are bunched accordingly, with the smallest equivalent width in the elastic group. The largest equivalent widths are in the plastic group, and the inelastic group falls between the elastic group and the plastic group. This behavior is expected because stress redistribution allows the equivalent width to increase with the amount of plastic material. As discussed previously, the equivalent widths of Dranger (1977), Otegui (1996) and Ballio et al. (1981) were derived for use with the plastic modulus, and the equivalent widths of AS 1418 (AS, 2001), CMAA (2008) and Ballio and Mazzolani (1983) were derived for use with the section modulus.

Because the equation developed by Ballio and Mazzolani (1983) is in very close agreement with the work of Jaramillo (1950), Timoshenko and Woinowsky-Krieger (1959) and the current finite element results in this paper, it will be regarded as the correct elastic curve. Therefore, all of the elastic research is represented with Equation 10.

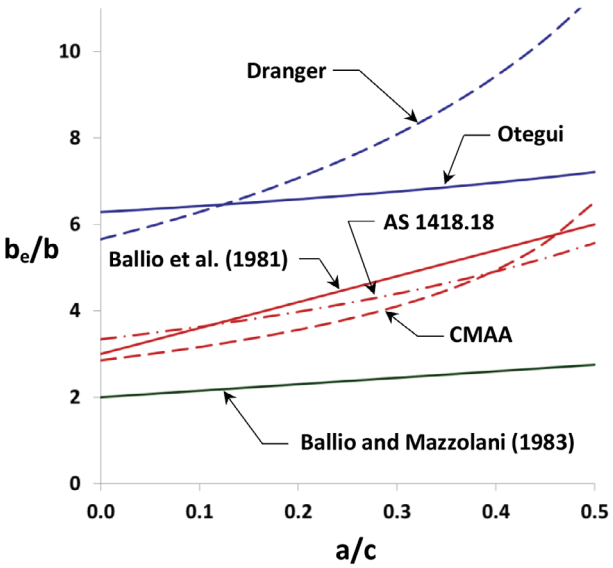

Fig. 8. Comparison of equivalent widths.

The equivalent widths implicit in the monorail design specifications (CMAA, AS 1418) are somewhat higher than the elastic values; it can be concluded then, that some inelastic deformation is required to reach the nominal strength. Although the equation of Ballio et al. (1981) was developed for use with the plastic modulus, it provides a reasonable linear approximation of the implied equivalent widths in the monorail design specifications, which use the section modulus.

For strength design, the equivalent width according Dranger (1977) is less than that of Otegui (1996) for small values of a/c. However, the difference between the two values is small, and Otegui's equation controls the design over most of the a/c range.

Design Recommendations for Equivalent-Width Equations

The design of flanges bent in single curvature can be separated into two groups: serviceability design and strength design. Serviceability design should be used where the flange must remain essentially elastic to prevent localized distortion, such as for monorail beams. Selection of the proper design philosophy is important because the plastic strength is more than four times the initial yield load. However, when the flange strength is calculated on the basis of a fully plastic yield line pattern, a deformation of approximately ¼ in. can be expected at the nominal load level (Dowswell, 2011).

In most cases of serviceability design, a limited amount of yielding can be allowed to accommodate some minor stress redistribution. The available equivalent-width equations in this inelastic group are from the design methods of Ballio et al. (1981), AS 1418 and CMAA. Because the three design methods in this group result in similar equivalent widths and the equation developed by Ballio et al. is the least complex, it is recommended for design. Therefore, Equation 11 is recommended for calculation of the nominal yield moment according to Equations 2 and 3. In rare cases, where even a small amount of inelastic deformation would be detrimental, Equation 10 can be used to calculate the equivalent width.

For strength design, both of the available equivalent-width equations were developed with the yield line method. Figure 8 shows that Otegui's (1996) yield line pattern controls the design over the practical range of a/c, and the equivalent width using Dranger's (1977) pattern is smaller only at very low a/c ratios. Therefore, Equation 23 is proposed for equivalent-width calculations using strength design. The nominal plastic moment is calculated with Equations 4 and 5.

STRESS INTERACTION

When the flange is subjected to longitudinal stress in addition to local bending stress, interaction of the stresses can reduce the local bending strength. Longitudinal stresses are typically caused by global strong-axis bending of the beam but can also be caused by axial loading and global bending about the weak axis of the beam. The quantification of this effect is complex due to the two-way local bending of the flange and the stress redistribution that occurs with increased load. The interaction of stresses has been the subject of several research projects, and it is addressed by the monorail design specifications.

Elastic Stress

Von Mises' criterion is accurate for predicting the initiation of yield in ductile metals when loaded by various combinations of normal stress and shear stress. For plane stress, von Mises' equation reduces to

$$\sigma_{ev} = \sqrt{\sigma_x^2 + \sigma_z^2 - \sigma_x \sigma_z + 3\tau^2} \tag{47}$$

where

σ_{ev} = effective uniaxial yield stress, ksi
σ_x = applied stress in the x-direction, ksi (tension positive)
σ_z = applied stress in the z-direction, ksi (tension positive)
τ = applied shear stress, ksi

If the shear stress is neglected, von Mises' equation can be expressed in the form of a reduction factor, α.

$$\alpha = \sqrt{1 - \frac{3n^2}{4}} - \frac{n}{2} \tag{48}$$

where

$$n = \frac{f_b}{F_y} \tag{49}$$

F_y = specified minimum yield stress of beam, ksi
f_b = longitudinal stress in the bottom flange of the beam, ksi

Inelastic Strength

For use with Equation 11, Ballio et al. (1981) suggested an elliptical interaction of the local bending strength of the flange and the longitudinal tension stress in the flange.

$$\left(\frac{f_b}{F_y}\right)^2 + \left(\frac{P}{P_n}\right)^2 \le 1.0 \tag{50}$$

where

P_n = nominal load calculated with Equations 1, 4 and 5, kips

Equation 50 can be expressed in the form of a reduction factor as

$$\alpha = \sqrt{1 - n^2} \tag{51}$$

Plastic Strength

When the main member carries axial compression, the plastic local bending strength is reduced. Cao, Packer and Yang (1998) reviewed the previous work on the reduction in strength due to normal stresses acting on the yield line pattern. They found that the reduction factor was dependent not only on the axial stress in the element containing the yield line pattern, but also on the geometry of the yield line pattern. In addition to developing a new equation, Cao et al. showed that Equation 52, originally developed by Kurobane (1981) for circular hollow sections, provides a conservative estimate of the strength reduction for elements with rectangular yield line patterns.

$$\alpha = 1 - 0.3 n_c \left(1 + n_c\right) \tag{52}$$

where

$$n_c = \frac{f_c}{F_y} \tag{53}$$

f_c = longitudinal compression stress in the element (compression positive), ksi

When the element carries axial tension, Cao et al. (1998) showed that the yield line strength is not reduced.

Monorail Design Specifications

Von Mises' criterion is specified in CMAA (2008) and for serviceability design in Eurocode (1999). For ultimate strength design, Eurocode specifies a reduction factor of

$$\alpha = 1 - \left(\frac{\gamma f_b}{F_y}\right)^2 \tag{54}$$

which can be simplified with the substitution of Equation 49.

$$\alpha = 1 - (\gamma n)^2 \tag{55}$$

To get a nominal reduction factor, set $\gamma = 1.0$, which gives

$$\alpha = 1 - n^2 \tag{56}$$

Australian Standard AS 1418 (AS, 2001) Section 5.12.3.1 specifies Equation 57.

$$\alpha F_y = F_y - 1.1 f_b \tag{57}$$

Equation 57 can be expressed in the form of a reduction factor and simplified with the substitution of Equation 49 to get Equation 58.

$$\alpha = 1 - 1.1n \tag{58}$$

If the 1.1 multiplier on n is assumed to be a partial safety factor, the nominal reduction factor is

$$\alpha = 1 - n \tag{59}$$

Summary and Conclusions for Stress Interaction

Figure 9 shows a plot of the reduction factor, α, versus the normalized longitudinal stress, n, for each of the reduction factor equations discussed in this paper. Von Mises' equation and the AS 1418 reduction factor are intended to ensure the material remains elastic. The remaining curves are for reductions in the inelastic and plastic strength. The curves show that the effect of longitudinal stress is more pronounced for elastic design than for plastic design.

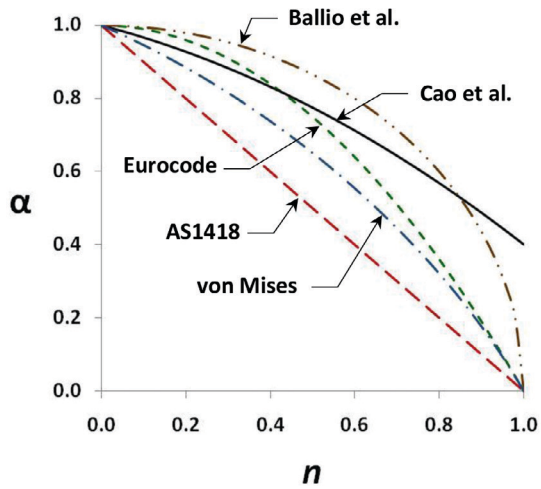

Fig. 9. Reduction factors for longitudinal stress in the bottom flange.

Design Recommendations for Stress Interaction

Reduction factors for stress interaction in serviceability design are intended to prevent large-scale yielding that would cause unacceptable deformations. The two reduction factors available for serviceability design were developed from AS 1418 and von Mises' criterion. It is well known that von Mises' criterion provides accurate results, and Figure 9 shows that the linear equation in AS 1418 provides conservative results compared to von Mises' criterion. Although von Mises' criterion is slightly more complex than the linear interaction in AS 1418, it provides a significant increase in strength for most values of n. Therefore, the additional complexity appears to be justified to obtain a more accurate solution. Equation 48 is proposed to estimate the strength reduction in the presence of longitudinal stress for serviceability design.

Reduction factors for stress interaction in strength design were presented by Cao et al. (1998), Ballio et al. (1981) and Eurocode. The equation by Cao et al. is the only method that has been proven accurate compared to tests and finite element models. The recommendations of Cao et al., which reduces the strength according to Equation 52, can be used to estimate the effect of longitudinal compression stress for strength design.

CLOSELY SPACED LOADS

Closely spaced loads are common at beam flanges supporting four-wheel monorail trolleys. This loading condition can also occur when two hanger rods are located close together. If the spacing between the loads is large enough, two separate failure patterns will form as shown in Figure 10a. In this case the strength is independent of the spacing. If the spacing is less than the critical spacing, a single failure pattern will form as shown in Figure 10b, which will cause a reduction in strength.

Monorail Design Specifications

CMAA (2008) and AS 1418 (AS, 2001) provide no specific guidance for closely spaced loads. However, Section 3.3.2.4.5 of CMAA requires that "consideration should be given to lower flange stresses which are not calculable by the formulae presented in section 3.3.2.4."

For design at service loads, Eurocode (1999) Section 5.5.2 (6) addresses closely spaced loads, where the spacing is less than $1.5b_f$: "Unless special measures are adopted to determine the local stresses, a conservative approach should be adopted by superposing the stresses calculated for each wheel acting separately." Eurocode strength design

provisions for closely spaced loads are based on Dranger's (1977) triangular yield line pattern.

Elastic Stresses

In addition to the maximum stresses in Table 1, Jaramillo (1950) also provided coefficients for stresses at intermediate locations in the *z*-direction along the flange. These coefficients were superimposed in a staggered pattern to calculate the maximum total stress at a point when two loads are applied. The results are expressed as a maximum stress ratio

$$k_s = \frac{\sigma_2}{\sigma_1} \tag{60}$$

where

σ_1 = stress caused by a single load, ksi
σ_2 = stress caused by two closely spaced loads, ksi

The k_s values for various combinations of *s*/*c* and *b*/*c* are listed in Table 3, where *s* is the spacing between loads.

In Figure 11, k_s is plotted versus *z*/*c* for *s*/*c* = 1, where *z* is the distance from the first load along the length of the beam. The shape of the curve is dependent on the *s*/*c* and *b*/*c* ratios. In some cases, the maximum stress occurs between the loads, as shown in Figure 11 for *b*/*c* = 1. In other cases, the maximum stresses occur at the same location as the loads, as shown in Figure 11 for *b*/*c* = 0.75 and less.

Figure 12 shows the stress ratio, k_s, versus the spacing ratio, *s*/*c*. At a spacing ratio of two, the stress ratio is negligible for the practical range of *b*/*c*. Therefore, the spacing effect can be neglected if the distance between adjacent wheel loads is less than the flange width. This leads to a critical spacing of

$$s_{ce} = 2c \approx b_f \tag{61}$$

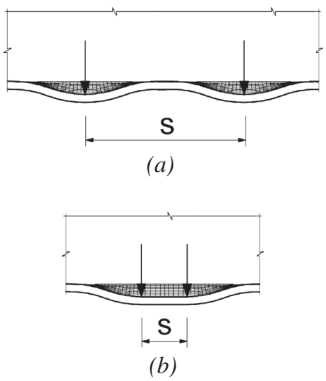

Fig. 10. Closely spaced loads: (a) actual spacing greater than critical spacing; (b) actual spacing less than critical spacing.

Relative to Equation 61, the critical end distance requirement in Eurocode (1999) is 50% conservative. For design of monorail beams, the geometry of most trolley/beam combinations will allow the spacing effect to be neglected.

When the actual spacing is less than the critical spacing, the reduction in strength can be accounted for by dividing the equivalent width for a single load by k_s from Table 3. The modified equivalent width for closely spaced loads is

$$b_{es} = \frac{b_e}{k_s} \tag{62}$$

For design, Equation 62 should be used to calculate the equivalent width if the actual spacing is less than the critical spacing. Otherwise, the spacing effect can be neglected.

Plastic Strength

For closely spaced loads, the plastic strength can be calculated using two half yield line patterns separated by the spacing between the loads as shown in Figure 13. The total equivalent width is calculated as the sum of the equivalent

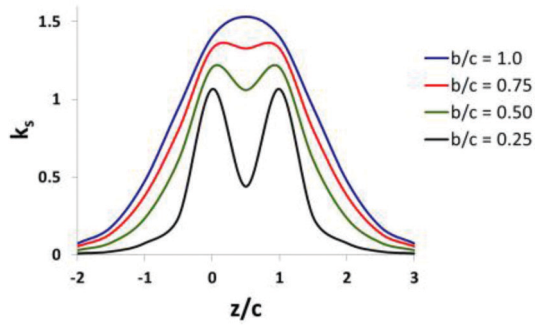

Fig. 11. k_s *versus* z/c *for* s/c = *1.*

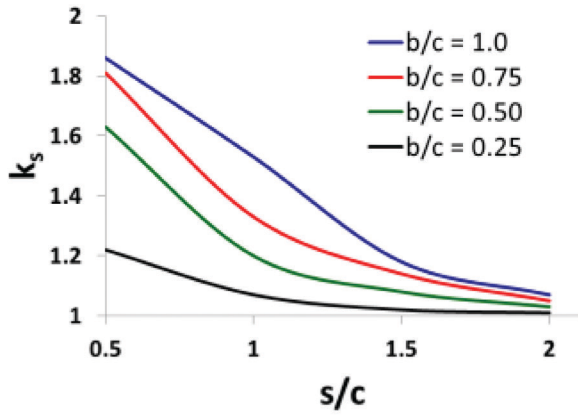

Fig. 12. k_s *versus* s/c.

Table 3. Values of k_s for Closely Spaced Loads				
s/c	b/c			
	1.0	0.75	0.50	0.25
0.50	1.86	1.81	1.63	1.22
1.0	1.53	1.33	1.20	1.07
1.5	1.18	1.14	1.08	1.02
2.0	1.07	1.05	1.03	1.01

width of the parabolic yield line pattern plus the distance between the loads, *s*. Adding *s* to b_e from Equation 23 and dividing by 2 to get the equivalent width per load, the plastic equivalent width is

$$b_{es} = 2b\left(\frac{\pi}{2}+\beta\right)+\frac{s}{2} \tag{63}$$

Because of the stress redistribution required to obtain the plastic strength, the critical spacing for strength design is larger than for serviceability design. The critical spacing is determined by setting Equation 63 equal to Equation 23 and solving for *s*, which results in Equation 64.

$$s_{cp} = 4b\left(\frac{\pi}{2}+\beta\right) \tag{64}$$

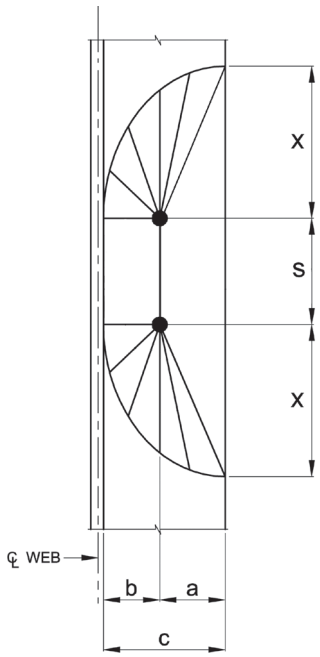

Fig. 13. Yield line pattern for closely spaced loads.

For design, Equation 63 should be used to calculate the equivalent width if the actual spacing is less than the critical spacing. Otherwise, Equation 23 should be used.

END LOADS

Although monorail beams typically have end stops (which keep the trolley away from the end of the beam), sometimes nonwelded splices are used (which creates a condition where the load acts at the beam end when the wheel rolls over the splice). Also, there are cases where hangers and other loads are applied near the end of the member. If the load is located beyond a critical distance from the end of the member, the strength will not be affected. However, the strength can be reduced substantially when the load is close to the member end.

Monorail Design Specifications

CMAA (2008) provides no specific guidance for loads near the end of monorail beams. However, Section 3.3.2.4.5 requires that "consideration should be given to lower flange stresses which are not calculable by the formulae presented in section 3.3.2.4."

For flanges that are free to displace at the end of the beam, AS 1418 (AS, 2001) Section 5.12.3.1 requires the flange thickness to be increased by 30% if the load is within $b_f + d$ of the end of the beam. This is an equivalent stress multiplier of $(1.3)^2 = 1.7$.

For serviceability design, Eurocode (1999) Section 5.5.2 (4) provides Equation 65 to calculate the flange bending stress when the load is at the end of the member.

$$\sigma = \left(\frac{P}{t_f^2}\right)\left[5.6-3.2\left(\frac{a}{c}\right)-2.8\left(\frac{a}{c}\right)^3\right] \tag{65}$$

Equation 65 neglects the effect of the distance from the load to the end of the member. Presumably, it was developed with the load at the end of the flange ($e = 0$), which is the worst case. Strength design provisions in Eurocode (1999) are based on the triangular yield line pattern derived by Dranger (1977).

Table 4. Values of k_e for Loads Near Member Ends				
e/c	*b/c*			
	1.0	**0.75***	**0.50***	**0.25***
0	2.60	2.84	3.09	3.11
0.125	2.28	2.35	2.26	1.79
0.250	1.97	1.92	1.81	1.30
0.375	1.74	1.67	1.46	1.15
0.500	1.55	1.45	1.26	1.09
0.625	1.38	1.29	1.16	1.05
0.750	1.26	1.19	1.11	1.04
0.875	1.19	1.13	1.08	1.03
1.000	1.13	1.09	1.06	—
1.125	1.09	1.07	1.04	—
1.250	1.06	1.05	1.03	—
1.375	1.04	1.03	—	—
1.5	1.03	—	—	—
* Only values of 1.03 and greater are listed				

Elastic Stresses

According to Equation 65, the stress due to end loads can be much higher than for intermediate loads. To determine the effect of the distance from the load to the end of the member, 44 finite element models were built using the modeling procedure described earlier. The models were proven accurate by comparison with the theoretical solutions of Jaramillo (1950) and Timoshenko and Woinowsky-Krieger (1959) and the finite element models of Ballio and Mazzolani (1983).

The *e/c* ratio varied from 0 to 1.5, where *e* is the distance from the load to the end of the member. Four *b/c* ratios were used: 0.25, 0.50, 0.75 and 1.0. The results are presented in Table 4 as a stress ratio, k_e.

$$k_e = \frac{\sigma_e}{\sigma_d} \tag{66}$$

where

σ_d = stress caused by a load not at a member end, ksi
σ_e = stress caused by a load near a member end, ksi

With the finite element results as a basis, it can be observed that the critical end distance in AS 1418 (AS, 2001) is extremely conservative. Conversely, the 1.3 factor for end-loaded flanges can be very nonconservative for $e/c < 0.375$.

Equation 65 from Eurocode (1999) agrees reasonably well (17% conservative on average) with Table 4 values at $e/c = 0$ and $b/c \geq 0.5$. Therefore, the equation can be used for end loaded monorail beams ($e = 0$). The most common case with $e = 0$ is nonwelded splices, where the wheel passes from one beam to the next. For monorail beams with angle end stops, where $e > 0$, Equation 65 can be extremely conservative.

The k_e values are plotted versus *e/c* in Figure 14. It may seem intuitive for design engineers to simply assume the equivalent width is reduced by 50% at the end of the beam (where $e = 0$). Figure 14 clearly shows that this is nonconservative because the stress increases by more than 200% when $b/c \geq 0.5$. The reason for k_e values > 2 can be better understood by observing the deformed shape of the flange. Figure 15a shows the deformed shape of a flange with an intermediate load and Figure 15b shows the deformed shape of an end-loaded flange. It can be seen that the end-loaded flange is in single curvature and the flange with the intermediate load is in double curvature. The flexural stiffness provided by the double-curvature bending spreads the equivalent width farther along the length of the flange, providing more strength.

For $e/c \leq 1.375$ and $b/c \geq 0.5$, which covers the most common cases, k_e can be calculated with Equation 67. This equation was developed by curve-fitting the data and adjusting the curve-fit equation upward to eliminate excessive nonconservatism. In the worst cases within the range of applicability, Equation 67 is conservative by 17% and nonconservative by 3%.

$$k_e = -1.85\left(\frac{e}{c}\right)^3 - 5.23\left(\frac{e}{c}\right)^2 - 5.24\left(\frac{e}{c}\right) + 3.03 \tag{67}$$

From observation of Table 4, the end distance effect can be neglected for all values of *b/c* if *e/c* is less than 1.375. This

leads to a critical end distance of

$$\begin{aligned} e_{ce} &= 1.38c \\ &\approx 0.7b_f \end{aligned} \tag{68}$$

For most monorail beams with angle end stops, the end stop leg width plus the wheel radius will be greater than $0.7b_f$. Therefore, in this case, the end-load effect is negligible.

When the actual end distance is less than the critical end distance, the reduction in strength can be accounted for by dividing the equivalent width for a single load by k_e. The modified equivalent width for serviceability design is

$$b_{ee} = \frac{b_e}{k_e} \tag{69}$$

Plastic Strength

The plastic strength of end-loaded flanges can be calculated using the yield line pattern in Figure 16. The equivalent width is half of the equivalent width of the parabolic yield line pattern plus the distance from the load to the end of the member. Adding e to $b_e/2$, where b_e is taken from Equation 23, the equivalent width is

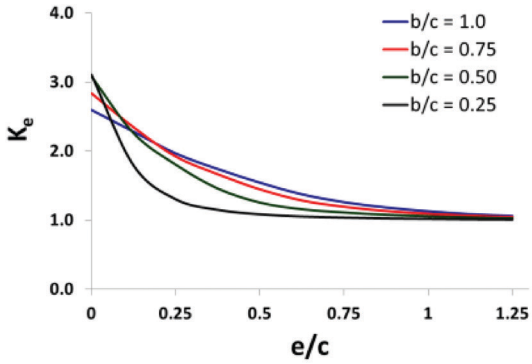

Fig. 14. k_e *versus* e/c.

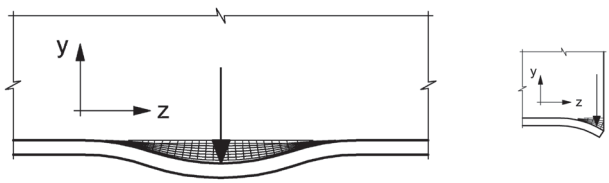

Fig. 15. Deformed shapes for double- and single-curvature bending: (a) double-curvature bending; (b) single-curvature bending.

$$b_e = 2b\left(\frac{\pi}{2}+\beta\right)+e \tag{70}$$

The critical end distance is determined by setting Equation 70 equal to Equation 23 and solving for e, which results in Equation 71.

$$e_{cp} = 2b\left(\frac{\pi}{2}+\beta\right) \tag{71}$$

For design, Equation 70 should be used to calculate the equivalent width if the actual end distance is less than the critical end distance. Otherwise, Equation 23 should be used.

For loads at the end of the member (e = 0), Eurocode (1999) specifies $b_e = 2c'$, which is much less than the equivalent width calculated with Equation 70. Because the other Eurocode provisions are based on a triangular yield line pattern, the equivalent width for a triangular pattern at the end of a beam will be derived. A yield line cannot develop along the free edge at the end of the beam; therefore, the triangular yield line pattern consists of a single skewed yield line as shown in Figure 17. This pattern can potentially control the design over the parabolic pattern due to the availability of only one of the three yield lines that are available for the full yield line pattern (Figure 5).

The external work is

$$W_e = P\delta \tag{72}$$

The internal work is

$$W_i = m_p\left(\frac{\delta}{b}\right)\left(x+\frac{2c^2}{x}\right) \tag{73}$$

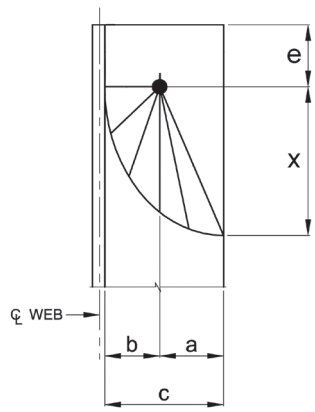

Fig. 16. Yield line pattern for loads near member ends.

where

x = width of the yield line pattern in the direction parallel to the beam length

Set internal work equal to external work and solve for P.

$$P = \left(\frac{m_p}{b}\right)\left(x + \frac{2c^2}{x}\right) \tag{74}$$

Determine the derivative of P with respect to x.

$$\frac{dP}{dx} = \frac{m_p}{b}\left(1 - \frac{2c^2}{x^2}\right) \tag{75}$$

Set $\frac{dP}{dx} = 0$ and solve for x.

$$x = c\sqrt{2} \tag{76}$$

Substitute x into Equation 74 to get the nominal load.

$$P_n = \frac{F_y t_f^2}{\sqrt{2}}\left(\frac{c}{b}\right) \tag{77}$$

Combining Equations 1, 4 and 77, the equivalent width is

$$b_e = 2c\sqrt{2} \tag{78}$$

This is half of the equivalent width of the full triangular pattern given by Equation 13, and the strength at the beam end is reduced by only 50% despite the loss of two of the three yield lines. This can be explained by noting that dimension x at the beam end is only half that of the full yield line, which provides a much smaller effective lever arm.

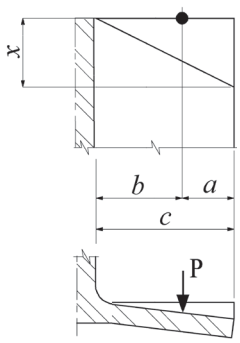

Fig. 17. Triangular yield line pattern at member end.

In conclusion, the plastic strength of a flange with a load at the end ($e = 0$) is equal to half of the strength of the full yield line pattern. This applies to the triangular pattern and the parabolic pattern in Figures 5 and 7, respectively. The conclusions from Figure 8 are valid at beam ends, and the parabolic pattern controls the design over most of the a/c range. Therefore, Equation 70 is recommended for strength design in all cases of end loading.

CONCLUSIONS

The equivalent-width method was explored in an effort to determine design procedures for elastic and plastic strength of flanges in single-curvature bending. The available procedures for designing flanges bent in single curvature were reviewed. New finite element models and yield line analyses were used to verify, expand and improve the existing design methods. Design recommendations were made for both the elastic and ultimate strength approaches. Recommendations were also made for interaction of the local bending strength with longitudinal stresses in the flange. The effects of closely spaced loads and loads acting near the ends of members were also addressed.

ACKNOWLEDGMENT

Thanks to Ed Marshall of Southern Company, who provided the interpretation of Hannover and Reichwald (1982).

SYMBOLS

F_y	Specified minimum yield stress, ksi
K_L	Load position factor
K_m	Equivalent width factor
P	Concentrated force, kips
P_a	Available wheel load, kips
P_n	Nominal load, kips
S_e	Section modulus of the equivalent beam, in.^{3}
W_e	External work, kip-in.
W_i	Internal work, kip-in.
Z_e	Plastic modulus of the equivalent beam, in.^{3}
a	Distance from the edge of the flange to the point of load application, in.
b	Horizontal distance from the face of the web to the concentrated load, in.
b'	Horizontal distance from the tangent point of the fillet radius to the concentrated load, in.

b_c Horizontal distance from the center of the beam to the wheel load, in.

b_e Equivalent width, in.

b_{ee} Equivalent width for end loads, in.

b_{es} Equivalent width per load for closely spaced loads, in.

b_f Flange width, in.

c Horizontal distance from the face of the web to the tip of the flange, in.

c' Horizontal distance from the tangent point of the fillet radius to the tip of the flange, in.

d Beam depth, in.

e Distance from the load to the end of the member, in.

e_{ce} Critical end distance for elastic design, in.

e_{cp} Critical end distance for plastic design, in.

f_b Longitudinal stress in the bottom flange of the beam, ksi

f_c Longitudinal compressive stress in the element in question, ksi

k_e Stress ratio for end-loaded flanges

k_s Maximum stress ratio for flanges with closely spaced loads

m_p Plastic capacity per unit length of yield line, kips

m_z Unit moment causing bending stress perpendicular to the length of the beam, kips

m_x Unit moment causing bending stress parallel to the length of the beam, kips

r Fillet radius, in.

t_a Flange thickness at the point of load application (for tapered flanges), in.

t_f Flange thickness, in.

t_w Web thickness, in.

s Spacing between loads, in.

s_{ce} Critical spacing for serviceability design, in.

s_{cp} Critical spacing for strength design, in.

x Width of the yield line pattern in the direction parallel to the beam length, in.

z Distance along the length of the beam, in.

α Reduction factor to account for longitudinal stress in the bottom flange due to global bending of the beam

α Half angle around the parabolic yield line pattern (Figure 7), radians

δ Virtual displacement of the load

γ Partial safety factor for LRFD design

θ Load distribution angle

σ_1 Stress caused by a single load, ksi

σ_2 Stress caused by two closely spaced loads, ksi

σ_d Stress caused by a load not at a member end, ksi

σ_e Stress caused by a load near a member end, ksi

σ_{ev} Effective uniaxial stress, ksi

σ_x Applied stress in the x-direction, ksi

σ_z Applied stress in the y-direction, ksi

τ Applied shear stress, ksi

REFERENCES

AS (2001), *Cranes, Hoists and Winches, Part 18: Crane Runways and Monorails*, Australian Standard, AS 1418.18-2001.

Ballio, G. and Mazzolani, F.M. (1983), *Theory and Design of Steel Structures*, Chapman and Hall.

Ballio, G., Poggi, C. and Zanon, P. (1981), "Elastic Plastic Bending of Plates Subjected to Concentrated Loads," *Joints in Structural Steelwork*, Proceedings of the International Conference held at Teeside Polytechnic, April 6–9, John Wiley and Sons

Cao, J.J., Packer, J.A. and Yang, G.J. (1998), "Yield Line Analysis of RHS Connections with Axial Loads," *Journal of Constructional Steel Research*, Vol. 48, pp. 1–25.

CMAA (2008), "Specifications for Top Running & Under Running Single Girder Electric Traveling Cranes Utilizing Under Running Trolley Hoist," Publication No. 74, Crane Manufacturers Association of America.

Dowswell, B. (2011), "A Yield Line Component Method for Bolted Flange Connections," *Engineering Journal*, AISC, Second Quarter, Vol. 48, No. 2.

Dranger, T.S. (1977), "Yield Line Analysis of Bolted Hanging Connections," *Engineering Journal,* AISC, Third Quarter, Vol. 14, No. 3.

Eurocode (1999), *Eurocode 3: Design of Steel Structures—Part 6: Crane Supporting Structures*, European Committee for Standardization.

FEM (1983), *Local Girder Stresses*, Federation Europeenne de la Manutention, FEM 9.341, First Edition, Section IX, Series Lifting Equipment.

Goldman, C. (1990), "Design of Crane Runway Girders for Top Running and Underrunning Cranes and Monorails," *Canadian Journal of Civil Engineering*, Vol. 17, pp. 987–1004.

Hannover, H. and Reichwald, R. (1982), "Local Flexural Stressing of Girder Lower Flanges, Part 1," *F&H,* No. 6, pp. 455–460 (in German).

Jaramillo, T.J. (1950), "Deflections and Moments Due to a Concentrated Load on a Cantilever Plate of Infinite Length," *Journal of Applied Mechanics*, ASME, Vol. 17, No. 1, March, pp. 67–72.

Kurobane, Y. (1981), *New Developments and Practices in Tubular Joint Design*, IIW Document XV-488-81, International Institute of Welding.

Mann, A.P. and Morris, L.J. (1979), "Limit Design of Extended End-Plate Connections," *Journal of the Structural Division*, ASCE, Vol. 105, No. ST3, March, pp. 511–526.

Otegui, M.A. (1996), *Simplified Method for Design of Stiffened and Unstiffened Structural Tee Hangers*, Master's Thesis, Virginia Polytechnic Institute, Blacksburg, VA.

Packer, J.A. and Morris, L.J. (1977), "A Limit State Design Method for the Tension Region of Bolted Beam-Column Connections," *The Structural Engineer*, Vol. 55, No. 10, October.

Timoshenko, S. and Woinowsky-Krieger, S. (1959), *Theory of Plates and Shells*, 2nd ed., McGraw-Hill, New York, NY.

Young, W.C. (1989), *Roark's Formulas for Stress and Strain*, 6th ed., McGraw-Hill, New York, NY.